Precast Concrete Industrial Portal Frames Subjected to Simulated Fire

Bruno Dal Lago[1](✉) (iD), Andrea Nicora[1], Paride Tucci[2], and Antonino Panico[2]

[1] Department of Theoretical and Applied Sciences, Università Degli Studi Dell'Insubria, Varese/Como, Italy
bruno.dallago@uninsubria.it
[2] Professional Fire Safety Engineer, Varese, Italy

Abstract. Precast concrete industrial frames made with tall columns cantilevering from their base and with simply supported prestressed horizontal beam/roof members, widely diffused in Europe and abroad, host most of the industrial activities of the continent, including the many characterised by high fire risk due to production or handling of materials/products having high combustion potential. The typical structural checks under fire action of such structures consists in a simplified cross-section analysis under the action of nominal temperature curves over time. However, this sort of analysis neglects the thermal-mechanical deformation induced by the exposure to fires of the structural elements. This contribution may become critical if considering the beam-column portal sub-assemblies, especially whenever peripheral columns are provided with infill walls. In this case, unlike central columns exposed to somehow uniform fire at all sides, a relevant differential thermal gradient occurs in the slender element, bringing it to large outward deformation activating 2nd order effects and coming into geometrical conflict with the beam, possibly leading to the collapse of the beam due to loss of support. This article presents a case study based on a real precast industrial building carried out employing a full Fire Safety Engineering workflow: (a) realistic fire scenarios encompassing different fire load distributions are simulated by computational fluid dynamics based on experimental curves of rate of heat release found in literature; (b) temperature distribution within the concrete elements was obtained with non-linear thermal analysis in variable regime; (c) strength and deformation of the concrete elements were checked with non-linear thermal-mechanical analysis based on parallel stripes in straight bending.

Keywords: Beam-column joints · Computational fluid dynamics · Fire Safety Engineering · Industrial buildings · Precast concrete · Thermal-mechanical analysis

1 Introduction

Industrial buildings are often more prone to fire exposure with respect to other facilities, mainly since many industrial activities involve high fire risk. Most of the heritage and novel industrial built environment in Europe is made by precast concrete frame structures

employing long-span pre-stressed members [1]. These elements are often designed, at least in Italy since the introduction of severe fire regulations in between 3 and 4 decades ago, according to strict requirements for fire resistance, to which they usually comply according to typical simplified design methods much easily than other structural materials. Apart from elementary table methods, typically the design of the main elements of the frame structures is carried out with analytical methods [2] employing sophisticated numerical tools to solve the cross-sectional equilibrium considering the deterioration of mechanical properties of the structural materials with nominal temperature evolution curves, sometimes including the thermal-induced strain in the solver [3–5]. Such an approach is typically carried out neglecting the deformation of the elements. Nevertheless, this assumption may result not being on the safe side for such typologies of structures, mainly due to the following two reasons: (a) often thin-walled folded-plate open sections are used for roof elements, which may distort under the temperature action [6, 7], and (b) the lengths of the structural elements may be remarkable, as well as their deformation under temperature exposure due to thermal gradients. The remarkable thermally-induced flexural deformation may lead to unexpected increase of deformation demand on roof connections, potentially leading to loss of support [7], and increment of second-order actions and effects. However, what stated above does not only apply for horizontal elements, but also for vertical ones, i.e. the columns. The columns of precast industrial frame buildings typically have compact cross-section (squared, squat-rectangular or circular) and are conceived as fixed at their base and hinged to the top beams. Thanks to the practical absence of moment transmission due to gravity loads from the roof, these columns are rather slender, and their deformability is also enhanced by their cantilever-based slenderness (shear span divided by cross-section side not seldom larger than 30), also drawing relevant second-order contributions affecting their lateral load capacity when displaced [8, 9].

The present paper focuses on the performance of precast concrete columns subjected to natural fire load evaluated in a real case study building. In particular, a full workflow of Fire Safety Engineering (FSE) [10, 11] was carried out according to the following steps: natural fire curves associated to realistic fire scenarios were assumed and modelled through Computational Thermal-Fluid-Dynamics (CTFD); temperature profiles were obtained in the structural elements through non-linear thermal transient analysis; advanced thermal-mechanical non-linear analysis was carried out to assess both stress state and deformation of the elements.

2 Precast Industrial Building at Study

The case study building is part of an industrial complex located in Northern Italy. The structure, originally built in the late 1990s, has a 20 m by 50 m rectangular plan and it is made with a precast concrete frame employing peripheral columns 6.8 m tall (above the industrial slab on grade) with compact square cross-section having 0.4 m of side supporting 20 m long double slope beams. The 5 m inter-axis between the beams is covered by slim T-shaped roof elements supporting a metal sheet. The geometry of the building is shown in Fig. 1. The roof is provided with four skylights and four strips of thermo-plastic low-melting translucid polycarbonate panels.
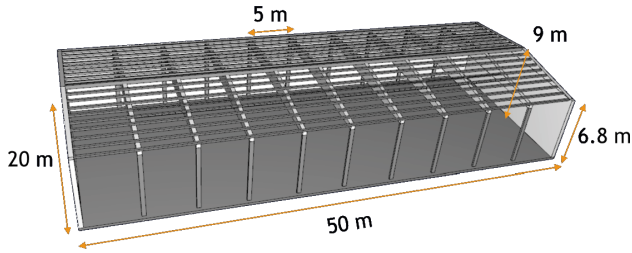
Fig. 1. Geometry of the building.

The building is used as a warehouse where paper material is stocked over industrial shelves (Fig. 2a). Masonry infill walls are provided in between the columns to clad the building (Fig. 2b). The column elements were analysed with sclerometre and cover-metre (Fig. 2c), in the context of a light and fast structural survey. The result was the identification of just $4\,\Phi18$ rebars (assumed to be made of steel FeB44k $-f_{yk} = 430$ MPa) with cover of 30 mm, one at each corner, and a good-quality concrete (estimated being of class C45/55 $-f_{ck} = 45$ MPa).

|		
(a)	(b)	(c)
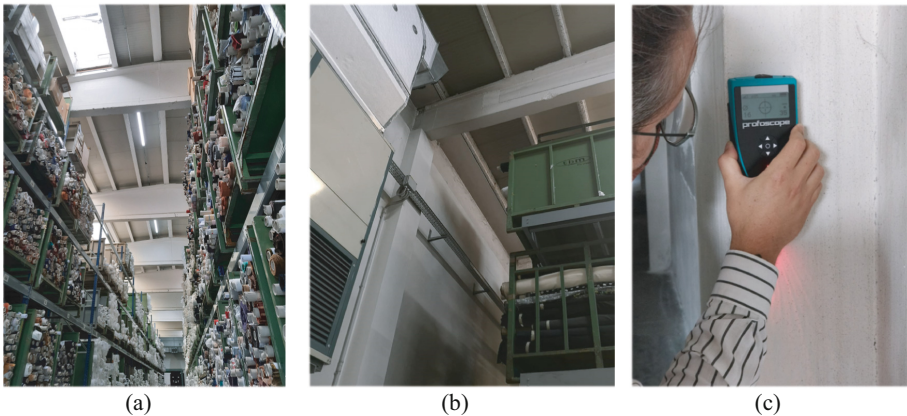
Fig. 2. Inspection of the building: (a) view of the combustible paper rolls piled in industrial shelves, translucent skylight and strips; (b) particular view of one column with infill cladding wall panel; (c) identification of the column reinforcement through cover-metre.

3   Fire Simulation

Realistic fire scenarios were simulated by computational thermal-fluid-dynamics. To this aim, the code FDS [12] was used in combination with the interface software PyroSim [13]. Firstly, the 3D geometric model of the compartment was developed (Fig. 3). All elements of both structure and cladding/cover of the building were simulated in the form of obstacles with their thermal properties. Also the thermal load associated with the

stored paper rolls was inserted following different scenarios. For the sake of brevity, a single scenario selected among those computed is presented hereafter.

The estimation of the Heat Release Rate (HRR) curve associated to the combustion of paper rolls was carried out as per Fig. 4 consulting experimental data available from oxygen consumption calorimetry tests on single paper roll specimens having dimensions of 1.6 m × 0.8 m × 1.2 m [14]. Each roll is characterised by an HRR curve having an ultra-fast trend, with a peak power equal to 4500 kW. For the definition of the total fire load of the activity, a total number of rolls equal to 456 was taken into account. Four rolls are arranged on 6 rows of 19 shelves. The model considers the ignition of a first roll with consequent propagation of the fire hearth to the surrounding ones. The ignition temperature of the paper was considered equal to 230 °C.
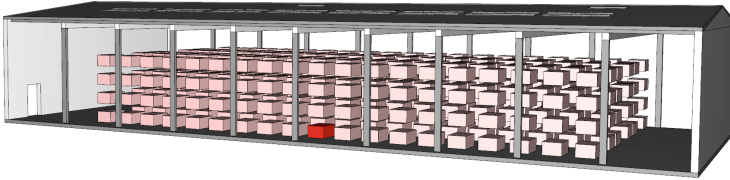
**Fig. 3.** Fire simulation numerical model. Ignition shelf in red.
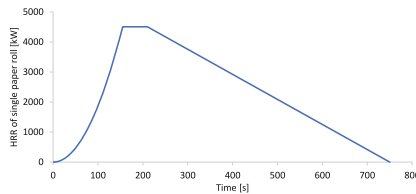
**Fig. 4.** Experimentally-calibrated HRR curve of single paper roll.

With the aim of finding a balance between the accuracy of the results and reasonable computation times, reference was made to the *D** criterion [15]. For the case study, the computational mesh consists of cells having either 1 cm, 2 cm, or 4 cm of characteristic dimension, respectively, the smaller size cells generated closer to the ignition location. The results of the analysis are synthetically shown in Fig. 5 in terms of resulting HRR curve and temperature distribution along the height of the column located in front of the firstly ignited shelf as measured by fictitious thermal couples inserted in the model. The curve clearly depicts that flashover did not occur in the growing branch, as expected due to the large volume of the compartment. After the plateau area, where fire burns at its maximum power also due to the ventilation flow ensured by melting of part of the translucent windows at around 700 s since ignition, the curve enters the self-extinction part with a marked descent mainly caused by reduction of the ventilation flow caused by the accumulation of smoke. Indeed, after about 1200 s since ignition, the rate of smoke production becomes higher than the speed with which the smoke itself is evacuated from the building through the openings installed in the ceiling. Consequently, excess smoke tends to "choke" the fire by displacing oxygen. As shown in Fig. 6, despite the translucid

polycarbonate windows located in the vicinity of the fire hearth appear melt allowing for abundant smoke and hot gas evacuation, accumulation of hot gases in all the environment progressively occurs through the fire. This, being in contradiction with the very efficient smoke evacuation evaluated in other analyses related to precast industrial buildings [7], shall be related to the relatively small skylight area in comparison with the environment volume.

The investigated column was subjected to temperatures ranging between 800 and 1150 °C for an exposure of about 20 min after about 5 min from first ignition, followed by a steep self-extinction branch.
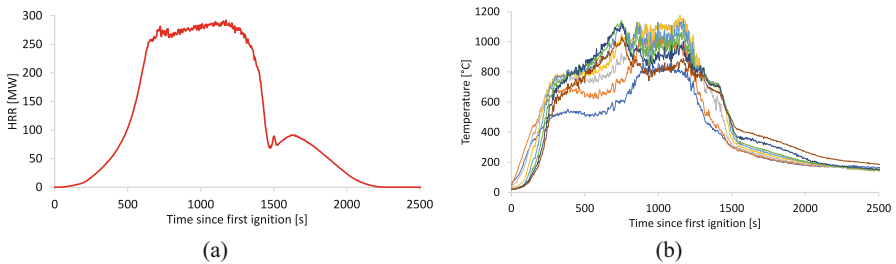
Fig. 5. Results of fire simulation: (a) output HRR curve; (b) temperature time history along the height of the investigated column.


investigated column
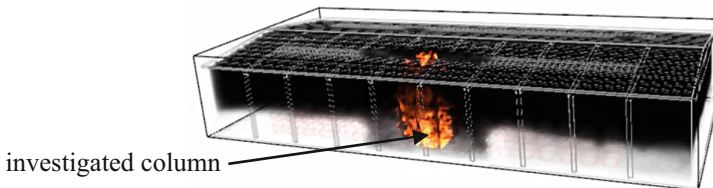
Fig. 6. Picture of the fire development after around 20 min from ignition.

4   Thermal Mapping of the Column Cross-Section

To map the temperature distribution in the structural elements, the most demanding temperature profile was selected. The thermal maps were evaluated according to a transient thermal analysis carried out with the finite element software Straus7 [16].

Following the instructions provided in Eurocode 2 [17], both convection and radiation thermal fluxes were considered in the surfaces of the elements, either exposed to fire (right) or to external temperature of 20 °C (left). The conductivity flux was evaluated by the finite element solver based on the thermally non-linear properties of concrete again described in [17], considering density, conductivity (curve 2), and specific heat (calcareous aggregates – 1.5% of base moisture). The thermal maps of the cross-section of the column element associated with the most severe thermal curve resulting in Fig. 5b

are shown in Fig. 7 for growing exposure times. It can be noted that the exposure surface considers the presence of the masonry cladding infill wall, the width of which was inserted in the model as an adiabatic boundary. As expected, the temperature rises rapidly in the exposed perimetre, concentrating the higher temperature in correspondence of the corners, exposed from two sides. In the meantime, most of the cross-section remains at very low temperature, also due to the direct exposure of the column to the external. This behaviour tends to minimise the global thermal elongation of the column element, although highly stimulating flexure due to the high temperature gradient between inner and outer sides.

(a)   (b)   (c)   (d)
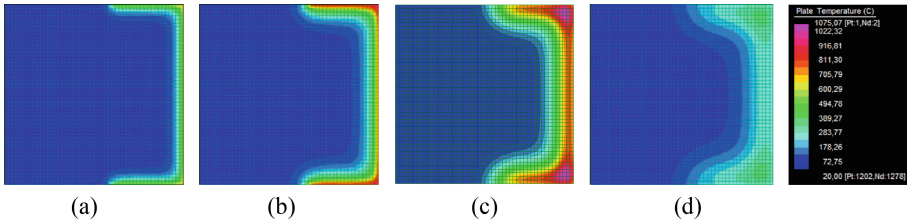
Fig. 7. Temperature distribution in the column cross-section after time exposure of: (a) 600 s; (b) 1200 s; (c) 1800 s; (d) 2400 s.

5   Thermal-Mechanical Analysis of the Column Element

The thermal-mechanical performance of the of the column was evaluated on the basis of a cross-sectional analysis [3–5, 7, 18] with the aims to: (a) check the demand over capacity ratio of the column when exposed to fire, and (b) check the kinematics of the column in fire, especially in terms of relative movements at the top with respect to the double-sloped beam. The material constitutive laws variable with temperature described in Eurocode 2 [17] were implemented in a self-written code in Mathcad 15 [19] following the characteristic material strengths described above, as shown in Fig. 8. It is reminded that the Eurocode 2 [17] constitutive law formulations consider implicitly the effect of transient creep [20].

   After having introduced the compacted geometry of the elements, the algorithm solves the sectional equilibrium equations of translation and rotation, as shown in Eq. 1 and 3, respectively. To be noted that the temperature in the column evolves in a 2D plane, both along the inner-outer and the transverse directions. Formally, the problem should be solved by adopting a resolution algorithm solving a bi-dimensional problem. However, a simplified assumption was made, resulting in a much easier solution algorithm, where the column cross-section was ideally divided into n stripes along the outer-inner direction. The temperature distribution was then derived based on output adjusting and interpolating operations for each stripe, as shown in Fig. 9 for a single time exposure. Finally, the problem was solved in straight bending following Eq. 1 and Eq. 2 by considering the n cross-sections in parallel. It is pointed out that this simplified procedure allows to fully account for the self-equilibrated stress generated by the thermal strain

in the direction of the procedure, as well as the resulting global sectional curvature and mean elongation, whilst it neglects this contribution in the transverse direction, which however is deemed not to mine the affordability of the results.
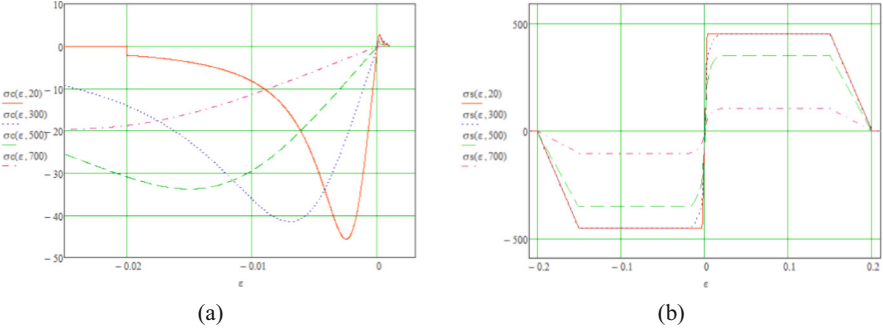
Fig. 8. Material constitutive laws in tension (+) and compression (−) as a function of the temperature following Eurocode 2 [17]: (a) concrete C45/55; (b) steel FeB44k. Stress in MPa.

$$N(\varepsilon_{ctop}, \chi) = \sum_{i=1}^{n} \left(\int_0^H \sigma_c\big(\varepsilon(y, \varepsilon_{ctop}, \chi) - \varepsilon_{c\theta}(\Delta\theta_n(y)), \Delta\theta_n(y)\big)\frac{b(y)}{n}dy \right)$$
$$+ \sum_{i=0}^{n_s} \sigma_s\big(\varepsilon(y_i, \varepsilon_{ctop}, \chi) - \varepsilon_{s\theta}(\Delta\theta(y_i)), \Delta\theta(y_i)\big)A(y_i) \tag{1}$$

$$M(\varepsilon_{ctop}, \chi) = \sum_{i=1}^{n} \left(\int_0^H \sigma_c\big(\varepsilon(y, \varepsilon_{ctop}, \chi) - \varepsilon_{c\theta}(\Delta\theta_n(y)), \Delta\theta_n(y)\big)\frac{b(y)}{n}(y - y_g)dy \right)$$
$$+ \sum_{i=0}^{n_s} \sigma_s\big(\varepsilon(y_i, \varepsilon_{ctop}, \chi) - \varepsilon_{s\theta}(\Delta\theta(y_i)), \Delta\theta(y_i)\big)A(y_i)(y_i - y_g) \tag{2}$$

where:
N is the external axial load; M is the external bending moment;
ε is the longitudinal strain; ε_{ctop} is the longitudinal strain of the top concrete chord;
χ is the sectional curvature; σ_c is the concrete longitudinal stress;
σ_s is the steel longitudinal stress; $\Delta\theta$ is the temperature gradient;
n_s is the number of steel rebar levels; H is the total depth of the concrete cross-section;
y is the coordinate through the thickness of the element starting from the external side;
n is the number of stripes in which the cross-section is divided;
$\varepsilon_{c\theta}$ is the thermal strain of concrete as defined by EC2 law;
$\varepsilon_{s\theta}$ is the thermal strain of steel as defined by EC2 law;
b is the chord width of the concrete cross-section;
y_g is the centre of gravity of the idealised cross-section;
A is the area of the steel rebars for a specific level.

The problem is defined by four variables, two of which are defined by the external loads (N,M) and the remaining two of which by the strain diagram $(\varepsilon_{ctop},\chi)$. By imposing

the external loads equal to the ones associated with the load condition in exceptional load combination (axial load N of 109.4 kN; no 1st order bending moment M) the system of two equilibrium equations can be solved finding out the two remaining variables, both associated to the strain diagram. This operation is carried out through the solution techniques implemented into the software.
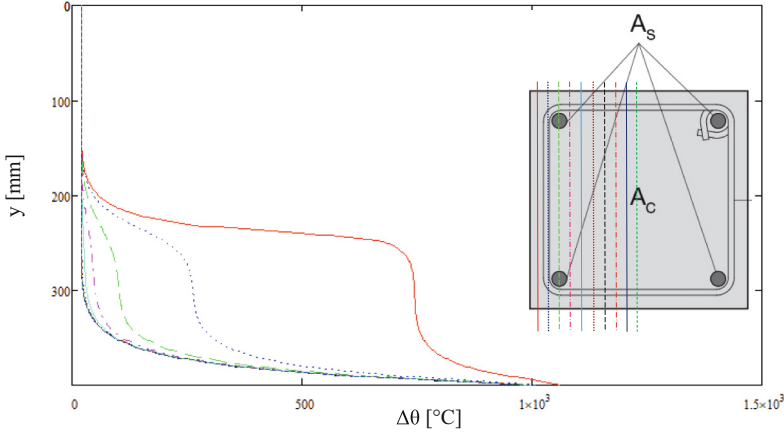
Fig. 9. Temperature functions for each 20mm-wide stripe for the single exposure of 20 min. Exposed side at bottom in figure and origin of y-axis at top in figure.

The results are reported in Fig. 10 for the selected exposure times of 10 and 20 min since first ignition. Due to the self-equilibrated stresses induced by thermal strain, a complex distribution of longitudinal stress takes place in the cross-section, with concrete being compressed at both inner and outer sides for only few centimetres, and tensioned in the inside, with internal cracking occurring behind the exposed side already at 10 min, and getting much expanded into the section at 20 min. The rebars appear being only moderately stressed. The evaluation of the sectional curvature allows to determine the flexural deflection of the elements through the resolution of the 2nd order differential equation shown in Eq. 3, where the curvature is defined including the 2nd order effects as a function of the column axial load N:

$$\frac{d^2v(x)}{dx^2} = -\chi\left(x, -Nv(x)\right) \tag{3}$$

where:

v is the flexural deflection as a function of both static and thermal loads;

x is the longitudinal coordinate.

The top deflection of the cantilever column appears being very relevant already after 10 min of exposure, where the integration of Eq. (3) neglecting the contribution of the axial force gives a 1st order lateral top displacement of 151 mm. Considering the 2nd order effects, the analysis provide 182 mm. This tendency goes towards divergence if considering the longer exposure time of 20 min, where top displacements of 398 mm and

654 mm are found if neglecting or considering the 2nd order effects, respectively. Indeed, this latter condition induces incipient collapse of the cantilever column due to 2nd order flexure. To be noted that the deflection becomes less pronounced with longer exposure time, mainly since the diffusion of temperature within the concrete element mitigates the thermal gradient. As an important side effect, such a large lateral deformation of the column may induce loss of support of the beam (Fig. 11) in all those diffused cases where the support length of the beam over the column is limited to around 20–30 cm, similarly as the current case study.

(a)   (b)
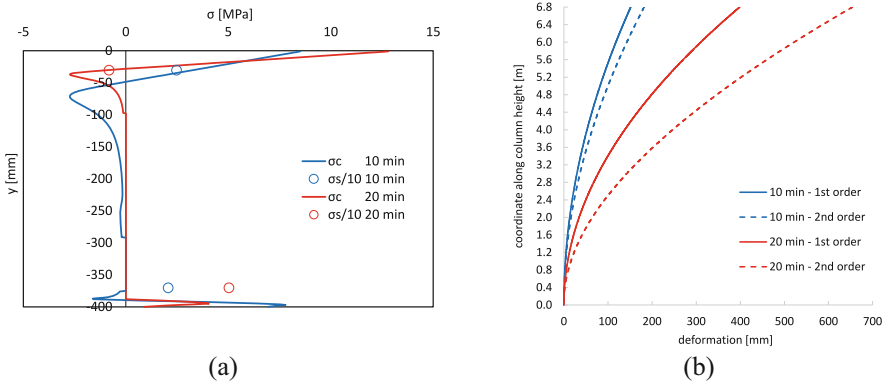
Fig. 10. Results of thermal-mechanical analysis: (a) mean 1st order stress distribution in the column along the inside-outside axis (tension (–) and compression (+)); (b) deformed shape associated to both 1st and 2nd order.
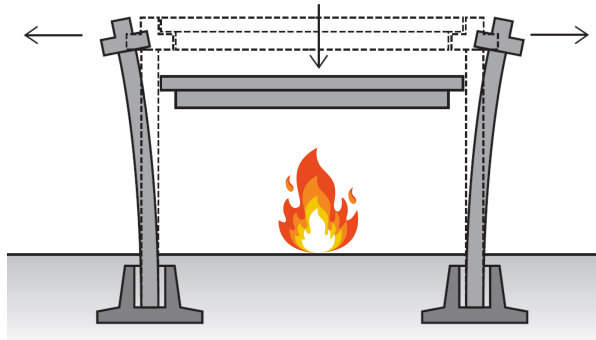
Fig. 11. Loss-of-support collapse mechanism of beam supported by edge columns highly deforming in fire.

6   Conclusions

The analysis shows that peripheral columns of precast industrial buildings are characterised by an intrinsic vulnerability when exposed to fire-induced thermal action, consisting in a very large deformation which may lead to failure of the column for 2nd

order effects or, much likely before, to the activation of loss-of-support mechanisms for the main frame beams. This tendency, which is not tackled in traditional simplified and advanced analysis methods in Fire Engineering, is caused by the large curvature resulting from elevated thermal gradients in the column, which becomes more pronounced for precast buildings with infill panels, representative of most of the existing industrial building stock dated up to around the 2000s. Future insights will be focused on studying the possible bracing effect arising from beam-to-columns connections other than simple sliding supports, indeed very diffused in existing buildings, i.e. typically dowels, although the entity of the column deformation attained by the simulation appears difficultly compatible with the capacity of those connections.

References

1. Dal Lago B (2017) Experimental and numerical assessment of the service behaviour of an innovative long-span precast roof element. Int J Conc Struct Mat 11(2):261–273
2. CEN – EN 1991–1–2 (2002) Eurocode 1: actions on structures, Part 1–2: general actions – actions on structures exposed to fire. European Committee for Standardization, Brussels, Belgium
3. Riva P, Franssen JM (2008) Non-linear and plastic analysis of RC beams subject to fire. Struct Concr 9(1):31–43
4. El-Fitiany SF, Youssef MA (2009) Assessing the flexural and axial behaviour of reinforced concrete members at elevated temperature using sectional analysis. Fire Saf J 44:691–703
5. Bamonte P, Kalaba N, Felicetti R (2018) Computational study on prestressed concrete members exposed to natural fires. Fire Saf J 97:54–65
6. Pedron A, Tondini N (2021) Fire behaviour of a prestressed thin-walled concrete v-beam. Fire Technol 58(1):353–378. https://doi.org/10.1007/s10694-021-01149-3
7. Dal Lago B, Tucci P (2023) Causes of local collapse of a precast concrete industrial roof after a fire event. Comput Concr 31(5)
8. Dal Lago B, Molina FJ (2018) Assessment of a capacity spectrum design approach against cyclic and seismic experiments on full-scale precast RC structures. Earthq Eng Struct Dynam 47(7):1591–1609
9. Bosio M et al (2023) Modelling and seismic response analysis of non-residential single-storey existing precast buildings in Italy. J Earthq Eng 27(4):1047–1068
10. Buchanan AH (Ed) (2001) Fire engineering design guide, 2nd Edition. centre for advanced engineering, University of Canterbury, Christchurch, New Zealand
11. Butcher K (Ed.) (2003) Fire engineering CIBSE guide. chartered institution of building services engineers, London, UK
12. McGrattan K, et al (2017) Fire Dynamics Simulator. NIST Special Publication 1019, 6th Edition
13. Thunderhead Engineering (2010) PyroSim: a model construction tool for fire dynamics simulator (FDS). PyroSim User Manual, Rel. 2010.2, Manhattan, USA
14. Hurley MJ, et al (2016) SFPE handbook of fire protection engineering. Springer, New York, USA. https://doi.org/10.1007/978-1-4939-2565-0
15. USNRC and EPRI (2007) Verification and validation of selected fire models for nuclear power plant applications, Volume 1: Main Report, U.S. nuclear regulatory commission, office of nuclear regulatory research (RES), Rockville, MD, and Electric power research institute (EPRI), Palo Alto, CA, NUREG- 1824 and EPRI 10 11999
16. G+D Computing (2010) Using Strand7 (Straus7) - Introduction to the Strand7 finite element analysis system system, Ed. 3, Strand7 Pty Limited, Sidney, Australia

17. CEN – EN 1992–1–2 (2004) Eurocode 2: Design of Structures, Part 1–2: General Rules-Structural Fire Design, European Committee for Standardization, Brussels, Belgium
18. Felicetti R, Gambarova PG, Meda A (2009) Residual behaviour of steel bars and R/C sections after a fire. Constr Build Mater 23:3546–3555
19. Parametric Technology Corporation (2010) Mathcad release 15.0, Needham, MA, USA
20. Franssen JM, Gernay T (2012) A formulation of the eurocode 2 concrete model at elevated temperature that includes an explicit term for transient creep. Fire Saf J 51:1–9